

# Digital Speckle Pattern Interferometry in Biomechanics: In Situ Inverse Analysis on Birds Beaks to Obtain Elastic Modulus of the Bony Core and the Keratin Layer

J. Soons, J. Dirckx, University of Antwerp, B

## Abstract:

The beak of finches is a very important example in evolution theory, and yet not fully understood. Furthermore, it is also fascinating from a mechanical point of view. In this paper we will use digital speckle pattern interferometry to obtain the displacement of the upper beak while loaded. Next, a finite element model is used in an inverse analysis, resulting in the modulus of the bony core and the keratin layer of this complex sample.

## Introduction

The mechanics of the beak play an important role in Darwin's evolution theory. Some beak morphologies seem to withstand larger forces better. Recently we introduced finite element (FE) modeling into this research [1]. The results of such studies are also interesting from a mechanical point of view. Indeed, the beak seems to rely on a highly optimized design: it needs to deal with large forces, but over-engineering will impede flying.

In order to build a realistic FE model, correct material parameters are needed [2]. The upper beak includes a bony core and a keratin layer. In literature a wide range of elasticity parameters for bone and keratin are defined [3]. In addition, it is very difficult to perform standard mechanical tests on small and complex biological samples. Indeed, besides the similarities between biomechanical and industrial research, such as the used techniques and the desired better understanding of the samples, one major difference exist: biological samples are not man-made. As a result it is very difficult to create for instance 'dog bone' samples for a standard tensile test. Consequently, we will use inverse modeling in this paper to obtain the elastic modulus of bone and keratin in situ. In the inverse analysis, the modulus of bone and keratin in the multi-parts FE model will be changed so a best fit with a digital speckle pattern interferometry (DSPI) experiment can be obtained. In a previous paper we compared DSPI with other techniques and we showed it merits [4].

## Material and methods

### DSPI Setup

The experimental setup is shown in fig. 1. We used a Michelson digital speckle pattern interferometry (DSPI) setup to obtain the out-of-plane displacement. As a result of the perpendicular illumination and viewing, we avoid shadow artefacts at the complex sample surface. A He-Ne beam ( $\lambda=632.8\text{nm}$ ) is expanded by a telescopic lens with a spatial filter. Next, the beam passes through a beam splitter and illuminates the upper beak of the finch and a reference plate. Both will show a speckle pattern resulting from their optical roughness and the use of coherent light. Both speckle patterns are subsequently back combined with the beam combiner, resulting in an interference pattern captured with a CCD camera (AVT, pike F-505) with a telecentric lens. Pearson's correlation of the interference pattern before and after a deformation results in the out-of-plane displacement. Between image recordings, four phase shifts of  $\pi/2$  are introduced by translating the reference plate (PI, S-303). From the phase shifted speckle interferograms, we can calculate full field displacement with a resolution of several tens of nanometers. We apply phase unwrapping and additional filtering before calculating the derivative of this out-of-plane displacement along the x-direction. This derivative is a more interesting parameter from a mechanical point of view. More details about this optical setup can be found in a previous paper [4].

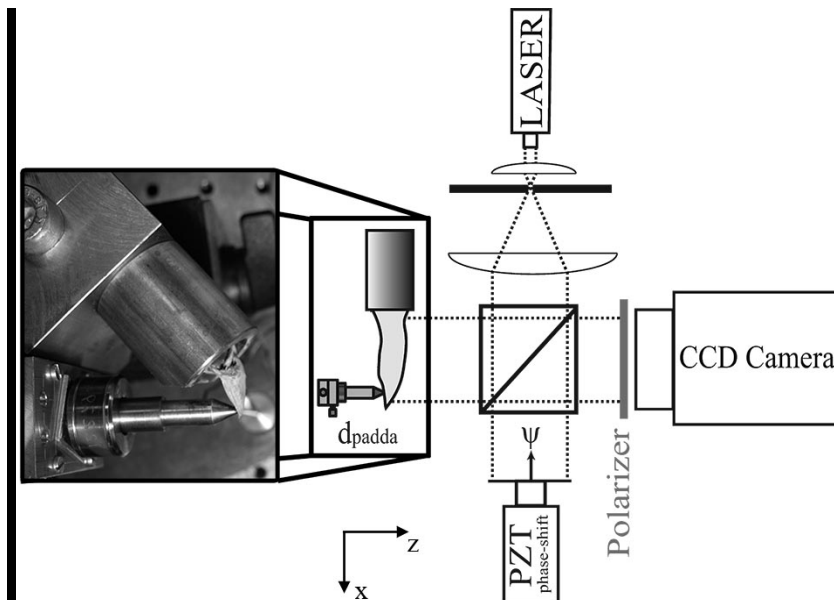


Fig. 1: Experimental setup: bending experiment and DSPI setup.

### Sample preparation, FE modeling and inverse analysis

Three Java finches (*Padda oryzivora*) were sacrificed using CO<sub>2</sub> gas. The back of the skull was cleaned by removing feathers, muscles and brain tissue. We also removed the lower beak so we can position an indentation punch (see fig. 1). Next, the skull and the jaw bones are constrained in a sample holder filled with polyester resin (VIAPAL 223BS/65). After a curing time of two days, we perform the bending experiment at three different locations at the bottom of the upper beak: at the center, at the tip where the bony core stops and totally at the tip. The indentation of approximately 3 μm is introduced with a stepper motor driven actuator (steps of 16 nm, PI M-235.2DG), the reaction force is measured with a load cell (Sensotec 31, 5N range) and the full field out-of-plane displacement on top of the upper beak is measured with DSPI (see above). The obtained displacement is divided by the reaction force. A coating and multiple measurements are used to improve the signal to noise ratio and to obtain better values for the derivative of the out-of-plane displacement in the x-direction.

A FE model of those bending experiments is also established. In the model, the jaw bones and the connection from the upper beak to the skull are constrained and the seed reaction force is introduced at the selected location. We also obtain the derivative of the out of-plane displacement along the x-direction on top of this beak. Those N values are linked to the corresponding DSPI results by a coefficient of determination R<sup>2</sup>:

$$R^2 = 1 - \frac{SS_{err}}{SS_{tot}}$$
$$SS_{err} = \sum_{i=1}^N (Exp(q_i) - FE(q_i))^2$$
$$SS_{tot} = \sum_{i=1}^N (Exp(q_i) - \overline{Exp})^2$$

$Exp(q_i)$  are the derivatives of the out-of-plane displacement along the x-direction obtained with DSPI at position  $q_i$ ,  $FE(q_i)$  are the same values for the FE model. R squared, closer to one indicates a better fit of the FE model to the DSPI measurement.

Finally we established surrogate models for the inverse analysis. The surrogate models link values for the modulus of bone and keratin in the FE model to a corresponding R squared. These models are created with the 'Matlab SUMO toolbox' [5]. We obtain a surrogate model for the three loading conditions separately (center, tip, total tip) and for the three loading conditions combined. Locating the maximum R squared in this surrogate model will results in the optimal modulus of bone and keratin in the selected domain.

## Results and discussion

The derivative of the out-of-plane displacement along the x-direction for a tip loading bending experiment is shown in fig. 2. In the left figure we present the results measured with the DSPI. As can be seen, we left out the bending area at the back of the beak ( $x < 6\text{mm}$ ) because it is difficult to model it correctly. In addition, we also left out a noisy part in the middle of the beak ( $x = \pm 12\text{mm}$ ). In the right figure we present the results for the FE model after full field optimization. We also present the cross-section results (fig. 3) for the three bending experiments of the specimen.

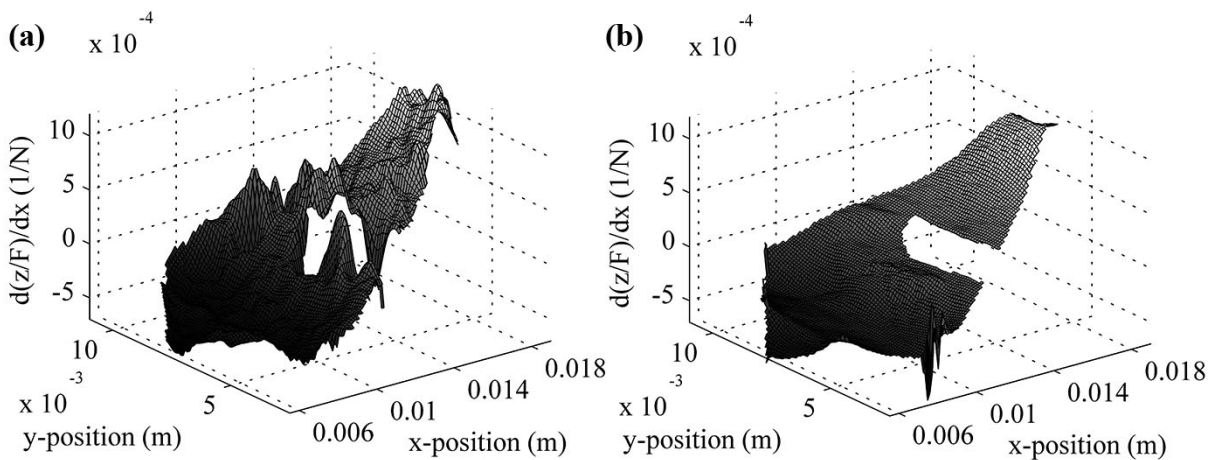


Fig. 2: Derivative of out-of-plane displacement (on top of the upper beak) along x-direction for padda 1. (a) obtained with DSPI, (b) the optimized FE result.

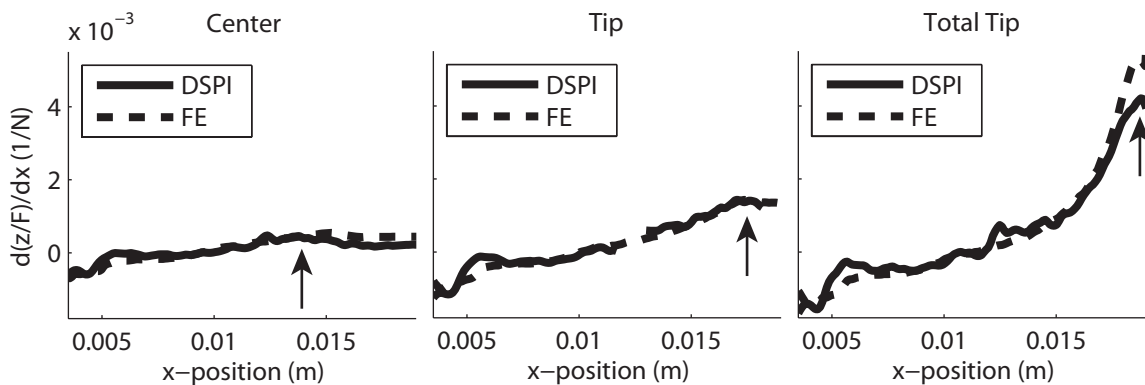


Fig. 3: Cross-section results ( $y=6\text{mm}$ ) for the derivative of the out-of-plane displacement along the x-direction for padda 1. DSPI measurements (full line) and FE results (dashed line) are shown for the three bending experiments (center, tip and total tip loading). We used the results of the combined optimization for the FE model ( $E_{\text{bone}} = 7.0\text{ GPa}$ ,  $E_{\text{keratin}} = 3.6\text{ GPa}$ , see table 1). The arrows indicate the indentation location.

As described above, surrogate modeling is used to acquire a best fit of the FE model to the DSPI measurement. As such we can obtain the optimal values for the elastic modulus of bone and keratin. Therefore we used three indentation locations (center, tip and total tip). The surrogate models of the three experiments are presented in fig. 4. We also show the model for the combined R squared. In the figure it is clear that some experiments have a different selectivity; e.g. for tip loading: a higher modulus for keratin can be compensated with a smaller modulus for bone. The combined surrogate model, however, has a superior selectivity.

Finally, the optimal elastic modulus acquired for the three tested samples are presented in table 1. For every specimen (padda 1, 2 and 3) we present the results with their corresponding R squared for the three loading experiments (center, tip and total tip). We also present the optimum obtained by combining the three bending experiments. It is clear that the total tip loading yield the best results of the three bending experiments. Indeed we obtain the highest R squared and the smallest variation between the results of the three samples. However, the variation of the combined results are even smaller due to the combination of the three different experiments with R squared as a weighting factor and due to the selectivity, seen in fig. 4.

By combining these results for the three Java finches, we obtain a modulus of  $(7.2 \pm 0.7)$  GPa for bone and  $(3.2 \pm 0.4)$  GPa for keratin. A high precision of approximately 10% is found and the values correspond with literature values [3].

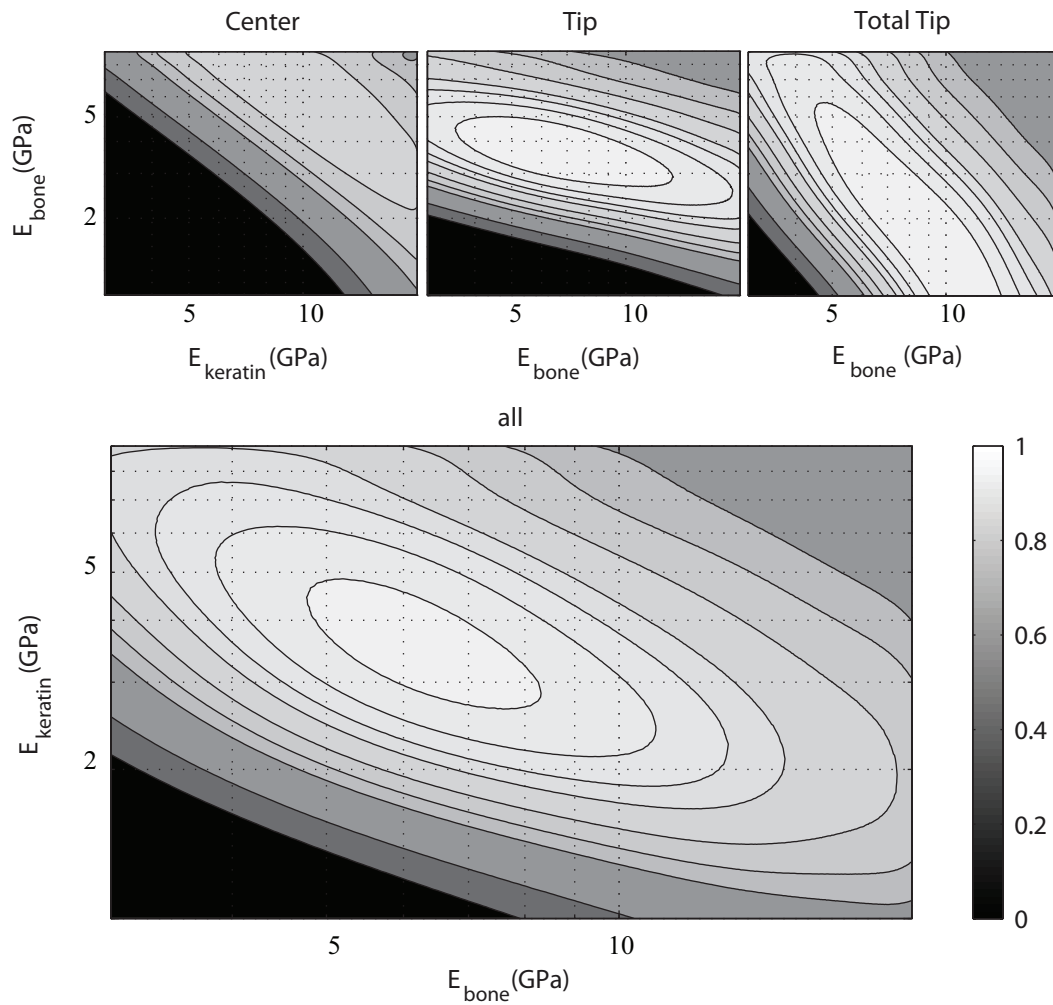


Fig. 4: Surrogate models, which link elastic moduli of bone ( $E_{bone}$ ) and keratin ( $E_{keratin}$ ) to a corresponding R squared value: center loading (top left), tip loading (top center), total tip loading (top right) and the combined surrogate model (bottom). Notice that we used a logarithmic scale.

Table 1: Optimal values obtained with an inverse analysis for the elastic modulus of bone ( $E_b$ ) and keratin ( $E_k$ ) with their corresponding  $R^2$ . The moduli are presented for three different test samples which are all tested on three different loading locations (center, tip and total tip). We also present the values of an inverse analysis which use the three loading experiments at the same time (combined).

	Center			Tip			Total tip			Combined		
	$E_b$	$E_k$	$R^2$	$E_b$	$E_k$	$R^2$	$E_b$	$E_k$	$R^2$	$E_b$	$E_k$	$R^2$
padda1	9.8	6.2	0.83	6.7	3.6	0.95	10	1.4	0.95	7.0	3.6	0.94
padda2	20	9.0	0.62	3	4.5	0.96	8.0	2.8	0.97	8.0	2.8	0.90
padda3	4.7	8.8	0.83	4.7	4.4	0.92	6.8	2.6	0.97	6.7	3.1	0.93

### Conclusion

DSPI can be used to measure deformations of complex biomechanical specimens such as the upper beak of a Java finch. An inverse analysis is introduced to obtain the modulus of the bony core and the keratin layer. The good correspondence with literature and the high precision of the obtained moduli indicates a well-functioning of the technique.

### Acknowledgements

Financial support to this project is given by the Research Foundation - Flanders (FWO).

## References

- [1] J. Soons, A. Herrel, A. Genbrugge, P. Aerts, J. Podos, D. Adriaens, Y. de Witte, P. Jacobs, and J. Dirckx, "Mechanical stress, fracture risk and beak evolution in Darwin's ground finches (*Geospiza*).," *Philosophical transactions of the Royal Society of London. Series B, Biological sciences*, vol. 365, Apr. 2010, pp. 1093-8.
- [2] D.S. Strait, Q. Wang, P.C. Dechow, C.F. Ross, B.G. Richmond, M.A. Spencer, and B.A. Patel, "Modeling elastic properties in finite-element analysis: how much precision is needed to produce an accurate model?," *Anat Rec A Discov Mol Cell Evol Biol*, vol. 283, Apr. 2005, pp. 275-287.
- [3] M. Meyers, P. Chen, a Lin, and Y. Seki, "Biological materials: Structure and mechanical properties," *Progress in Materials Science*, vol. 53, Jan. 2008, pp. 1-206.
- [4] J. Soons and J.J.J. Dirckx, "Full field displacement and strain measurement of small complex bony structures with digital speckle pattern interferometry and shearography," *Proceedings of the SPIE - The International Society for Optical Engineering*, Florianopolis: 2010, p. 73870C (10 pp.).
- [5] J. Aernouts, I. Couckuyt, K. Crombecq, and J.J.J. Dirckx, "Elastic characterization of membranes with a complex shape using point indentation measurements and inverse modelling," *International Journal of Engineering Science*, vol. 48, Jun. 2010, pp. 599-611.